26 *KSME International Journal, Vol. 13, No. 1, pp. 26~33, 1999*

Sliding Mode Control of a Shear-Mode Type ER Engine Mount

Seung-Bok Choi* and Young-Tai Choi*

(*Received April 15, 1998*)

This paper presents feedback control characteristics of a shear-mode type electro-rheological (ER) engine mount. The field-dependent yield stress of an arabic gum-based ER fluid is obtained using a couette type electroviscometer, and it is incorporated into the governing equation of motion of the ER engine mount, which is derived from a bond graph model. A sliding mode controller which directly represents the field-dependent damping force is formulated by taking into account the stiffness and damping properties of the system as parameter uncertainties. The controller is then experimentally realized by imposing a semi-active actuating condition. The effectiveness of the proposed ER engine mount is demonstrated showing capabilities of isolating the vibrations due to sinusoidal and random excitations.

Key Words: Electro-Rheological Fluid, Shear-Mode, Engine Mount, Vibration Suppression, Sliding Mode Control, Semiactive Actuator

1. Introduction

Along with the trend of consumers demands toward higher class of passenger cars, in recent years there has been an increasing demand to improve the noise and vibration characteristics of the vehicles. An automotive engine is one of the most dominant noise and vibration sources because it rotates itself and transmits the torque through a driveline. Therefore, in order to resolve vibration and noise problems due to the dynamic motion of the engine, numerous types of engine mounts have been and being proposed. One approach to devise engine mount is to utilize an electro-rheological(ER) fluid which has field-dependent Bingham characteristics.

The ER engine mount may be classified into three different types depending upon the working mode of the ER fluid actuator; flow-mode, shear-mode and squeeze-mode. Duclos (1987) proposed a tunable flow-mode ER engine mount that has multiple inertia paths containing the ER valves which could be used to control the fluid flow passing through the paths. Ushijima *et al.* (1988) proposed a flow-mode ER engine mount showing that it could be mechanically modeled as a single degree of freedom system. Petek *et al.* (1988) proposed a flow-mode ER engine mount with plate type electrodes and experimentally demonstrated its performance superiority over conventional hydraulic engine mount. Morishita *et al.* (1992) manufactured a flow-mode ER engine mount with plate type electrodes and undertook experiments by changing design parameters such as electrode gap. Williams *et al.* (1993) proposed a squeeze-mode ER engine mount. They derived an analytical model for the proposed ER engine mount and compared simulated results with experimental ones in order to prove the validity of the proposed model.

As evident from these previous works, most of researches concern with the flow-mode ER engine mount. However, this type of ER engine mount may cause performance deterioration for vibration isolation in the relatively high frequency and small amplitude of excitations. This is arisen from a so-called lock-up state between

* Smart Structures and Systems Laboratory Department of Mechanical Engineering Inha University Incheon 402-751, Korea, Http://sss̄lab. inha. ac. krK

electrode gaps. In the lock-up state, the flow motion of the ER fluid between electrodes does not take place. Instead the ER fluid behaves just like a solid. On the other hand, the squeeze-mode ER engine mount may have a difficulty of controlling the electric field in large amplitude of excitation due to the variation of the electrode gap. Furthermore, the variation of the electrode gap during the motion is unwelcome in the synthesis of real-time feedback control system. Consequently, the main contribution of this work is to propose a shear-mode ER engine mount to resolve above-mentioned problems, and to show how the proposed ER engine mount can be satisfactorily performed for vibration isolation. The effectiveness is evaluated by experimental realization.

The governing equation of motion of the shear-mode ER engine mount is derived via the bond graph method. The dynamic equation includes a control variable which is the field-dependent damping force obtained from Bingham model of the arabic gum-based ER fluid. A sliding mode controller associated with the control variable is formulated by treating the stiffness and damping properties of the system as parameter uncertainties. The controller is then experimentally realized by imposing a semi-active condition. Control responses are presented in both the frequency and time domains in order to demonstrate the effectiveness of the proposed ER engine mount.

2. Yield Stress of the ER Fluid

Rheological properties of ER fluids are reversibly changed depending upon the imposition of the electric field. The characteristics of ER fluids is changable from Newtonian flow in which particles move freely to Bingham behavior in which particles are aligned in chains by applying the electric field to the fluid domain.

Under the electric potential, the constitutive equation for the ER fluid is a form of Bingham plastic behavior expressed as

$$\tau = \eta \dot{\gamma} + \tau_y(E)\,\mathrm{sgn}(\dot{\gamma}) \qquad (1)$$

where τ is shear stress, $\dot{\gamma}$ is shear rate, η is viscosity, $\tau_y(E)$ is yield shear stress of the ER fluid, and sgn$(\cdot)$ is a signum function. $\tau_y(E)$ in Eq. (1) is a function of the electric field E and exponentially increases with respect to the electric field (Jordan and Shaw, 1989). Therefore, Eq. (1) can be represented by

$$\tau = \eta \dot{\gamma} + \alpha E^{\beta}\mathrm{sgn}(\dot{\gamma}) \qquad (2)$$

where the proportional coefficient, α and the exponent, β are intrinsic values of the ER fluid, which are functions of applied electric field, particle size, particle shape and concentration, carrier liquid, water content, temperature, and polarization factors such as particle conductivity. From Eq. (2), it is known that the shear stress is a function of the shear rate as well as the electric field.

The intrinsic values α and β of the ER fluid are usually obtained by experiments. In this study, a couette type electroviscometer is employed to obtain Bingham property of the ER fluid. For the ER fluid, arabic gum and transformer oil are chosen as particles and liquid, respectively. The size of particles ranges from 26μm to 88μm. The weight ratio of the particles to the ER fluid is 55%. Fig. 1 presents Bingham property of the ER fluid at 20℃. The shear stress in Fig. 1(a) is measured applying the electric field from 0kV/mm to 2kV/mm at each 0.5kV/mm, while the shear rate is increased up to 600 1/s. The measured field-dependent yield shear stress is used to get a linear regression and then, from the intercept at zero shear rate, the dynamic yield shear stress of the ER fluid is evaluated. Fig. 1(b) presents the distilled field-dependent yield shear stress. As can be seen from the figure, it is known that the yield shear stress increases exponentially with respect to the electric field. The yield shear stress $\tau_y(E)$ is obtained experimentally as follows: 297 $E^{1.46}$ Pa in the form of Eq. (2). Here the unit of E is kV/mm. Note, from the current density-electic field curve in Fig. 1(c), that the power required to get the yield shear stress is very low at 20℃.

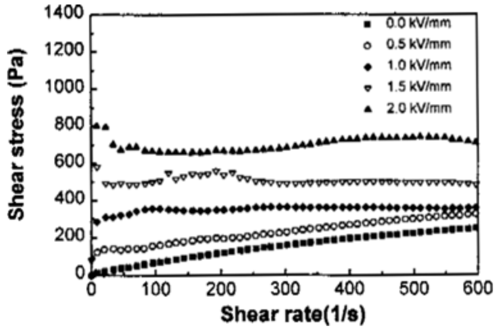

(a) shear stress

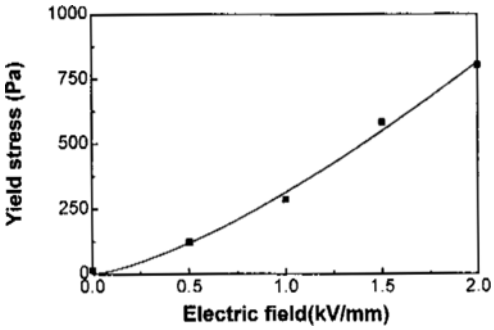

(b) yield stress

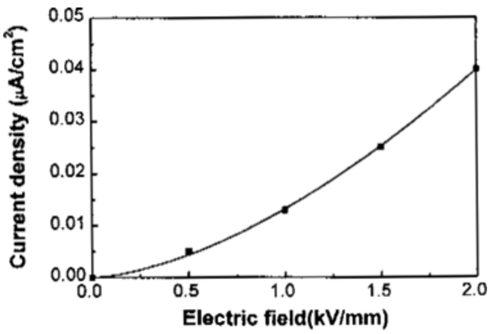

(c) current density

Fig. 1 Bingham property of the employed ER fluid.

3. Dynamic Modeling

The schematic configuration of the shear-mode ER engine mount proposed in this study is shown in Fig. 2. Multi-cylindrical electrodes which are fixed in parallel to the upper and lower plates move vertically when excitation is applied. This vibratory motion results in the shear type of the working mode of the ER fluid. The linear bearing is used to keep the electrode gaps constant during

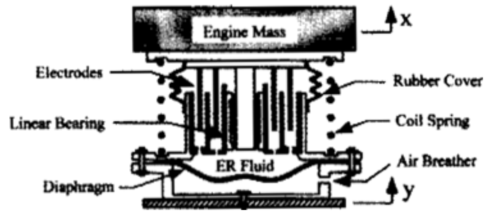

Fig. 2 Configuration of the shear-mode ER engine mount.

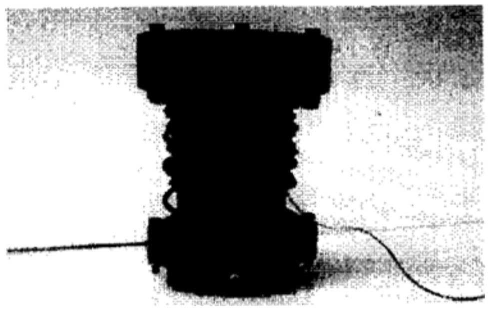

Fig. 3 Photograph of the shear-mode ER engine mount.

vertical motion. The number of the electrode gaps are 4. In order to prevent the ER fluid from spilling out of engine mount, rubber cover is arranged between the upper and lower plates. The volume enclosed by the rubber cover and diaphragm is filled with the ER fluid. In addition, the diaphragm is used to accumulate the flow pumped by the upper plate. The engine mass is attached to the upper plate and the frame is attached to the lower plate. Between the upper and lower plates, the coil spring is installed in order to support the engine mass. The positive (+) voltage of high voltage amplifier is connected to the lower electrodes, while the negative (−) voltage is connected to the upper electrodes. The photograph of the ER engine mount is shown in Fig. 3.

It is assumed that the ER fluid is incompressible. In addition, since the time response of the ER fluid is known to be very fast in the order of a few milliseconds, the dynamic model of the ER fluid itself is not considered. In order to obtain the governing equation of the ER engine mount, a bond graph model is built as shown in Fig. 4. From the bond graph model, the type and the flow of the energies existing in the engine mount

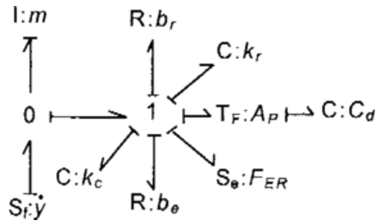

Fig. 4 Bond graph model of the ER engine mount.

can be identified, and thus the mathematical model can be directly derived (Rosenberg and Karnopp, 1983). In the case of the hydro-mechanical system it is relatively easy to derive the governing equation of the system without confusion. In this figure, m, k_r, k_c and C_d are the engine mass, the stiffness of the rubber, the stiffness of coil spring, and the compliance of the diaphragm, respectively. A_p is the piston area of the upper plate, b_r is the damping coefficient of the rubber, and b_e is the damping coefficient due to fluid resistance of electrode gap. The total shear stress of the system can be expressed by

$$\tau=\eta\frac{\dot{x}-\dot{y}}{h}+\alpha\left(\frac{V}{h}\right)^{\beta}\operatorname{sgn}(\dot{x}-\dot{y}) \quad (3)$$

where, h is the electrode gap and V is the applied voltage. The variables $\dot{x}$ and $\dot{y}$ are velocities of the engine mass and excitation, respectively. Integrating Eq. (3) with respect to the electrode area, we can obtain the total damping force F_t as follows:

$$\begin{aligned}F_t&=2\pi\sum_{i=1}^{N_n}r_i\eta\frac{L}{h}(\dot{x}-\dot{y})+2\pi\sum_{i=1}^{N_n}r_iLr\left(\frac{V}{h}\right)^{\beta}\\&\quad\operatorname{sgn}(\dot{x}-\dot{y})\\&=b_e(\dot{x}-\dot{y})+F_{ER}\end{aligned} \quad (4)$$

where, F_{ER} is the field-dependent damping force due to the yield shear stress of the ER fluid. It is known that the damping force F_{ER} can be continuously controlled by the properly applied electric field (Choi *et al.*, 1998). In Eq. (4), L is the electrode length and r_i is the effective radius of the electrode.

Now, from the bond graph model shown in Fig. 4, the governing equation of motion of the ER engine mount can be directly obtained as follows:

$$m\ddot{x}+b(\dot{x}-\dot{y})+k(x-y)=-F_{ER} \quad (5)$$

where, $b=b_r+b_e$ and $k=k_r+k_c+A_p^2/C_d$. The governing equation is rewritten in a matrix form as follows:

$$\dot{\mathrm{X}}=\mathrm{AX}+\mathrm{B}u+\mathrm{D} \quad (6)$$

where, $\mathrm{X}=[x\ \ \dot{x}]^T$, $u=F_{ER}$

$$\mathrm{A}=\begin{bmatrix}0 & 1\\ -\frac{k}{m} & -\frac{b}{m}\end{bmatrix}\quad \mathrm{B}=\begin{bmatrix}0\\ -\frac{1}{m}\end{bmatrix}$$

$$\mathrm{D}=\begin{bmatrix}0\\ \frac{k}{m}y+\frac{b}{m}\dot{y}\end{bmatrix} \quad (7)$$

4. Sliding Mode Control

The sliding mode control which has inherent robustness to system uncertainties is adopted to suppress the vibration due to excitations. In practice, it is hard to get accurate values of the stiffness and damping properties of the system. Therefore, these parameters need to be treated as the structured uncertainties as follows (Leitmann, 1981):

$$\begin{aligned}k&=k_0+\delta k,\ |\delta k|\le\rho_1 k_0\\ b&=b_0+\delta b,\ |\delta b|\le\rho_2 b_0\end{aligned} \quad (8)$$

where, k_0 and b_0 are the nominal stiffness and damping coefficient, and δk and δb are corresponding deviations. Note that the variations of the δk and δb are bounded by the weighting factors ρ_1 and ρ_2, respectively. By substituting Eq. (8) into the stiffness and damping coefficients in Eq. (7), the dynamic model can be expressed as

$$\dot{\mathrm{X}}=(\mathrm{A}_0+\Delta\mathrm{A})\mathrm{X}+\mathrm{B}u+\mathrm{D}_u \quad (9)$$

where, A_0 is the nominal part, $\Delta\mathrm{A}$ is the uncertain part, and D_u is the disturbance(excitation) including the parameter uncertainties. The magnitudes of the excitation displacement and velocity are assumed to be bounded as $|y|<\Psi_1$ and $|\dot{y}|<\Psi_2$, respectively.

Since the ultimate goal is to regulate the vibration of the uncertain system (9), we define the following sliding surface.

$$s=Cx+\dot{x},\ C>0 \quad (10)$$

where, C is the sliding surface gradient. The condition for existence of the sliding motion in the vicinity of the sliding surface $s=0$ is given by

$$s\dot{s}<0 \tag{11}$$

Then the system is subjected to be attracted to the sliding surface during the sliding motion, and hence has invariance properties against the external disturbance and parameter uncertainties. Now, we propose the following controller for the uncertain system (9).

$$u=mC\dot{x}-k_0x-b_0\dot{x}+k_g\mathrm{sgn}(s) \tag{12}$$

where, $k_g=\rho_1k_0|x|+\rho_2b_0|\dot{x}|+(1+\rho_1)k_0\Psi_1+(1+\rho_2)b_0\Psi_2$. Then, we can show that the uncertain system (9) with the proposed controller (12) satisfies the sliding condition (11) as follows:

$$\begin{aligned} s\dot{s}&=s\left\{C\dot{x}-\frac{k_0+\delta k}{m}x-\frac{b_0+\delta b}{m}\dot{x}+\frac{k_0+\delta k}{m}y\right.\\ &\quad\left.+\frac{b_0+\delta b}{m}\dot{y}-\frac{u}{m}\right\}\\ &=s\left\{\left[-\frac{\delta k}{m}x-\frac{\rho_1k_0}{m}|x|\mathrm{sgn}(s)\right]\right.\\ &\quad+\left[-\frac{\delta b}{m}\dot{x}-\frac{\rho_2b_0}{m}|\dot{x}|\mathrm{sgn}(s)\right]\\ &\quad+\left[\frac{k_0+\delta k}{m}y-\frac{(1+\rho_1)k_0}{m}\Psi_1\mathrm{sgn}(s)\right]\\ &\quad\left.+\left[\frac{b_0+\delta b}{m}\dot{y}-\frac{(1+\rho_2)b_0}{m}\Psi_2\mathrm{sgn}(s)\right]\right\}<0 \end{aligned} \tag{13}$$

It is noted that in practice, it is not desirable to use the discontinuous control input (12) because of the chattering. Therefore, we may replace sgn (s) in Eq. (12) by a saturation function with an appropriate boundary layer width of ε (Choi *et al.*, 1995).

The sliding mode controller given by Eq. (12) is designed for an active actuating device. However, the proposed ER engine mount is a semi-active one. Therefore, the control input force generated by the ER engine mount should satisfy the following condition.

$$u=\begin{cases}u & for\ u(\dot{x}-\dot{y})>0\\ 0 & for\ u(\dot{x}-\dot{y})\le 0\end{cases} \tag{14}$$

This semi-active condition physically implies that the control scheme in the semi-active mode only assures the increment of energy dissipation (Leitmann, 1994). Once the damping force u is determined, control voltage to be applied to the ER engine mount can be determined from the second term of Eq. (4). Note that the sliding mode condition given by Eq. (11) is not satisfied when $u(\dot{x}-\dot{y})\le 0$. This implies that as time goes on the sliding surface s does not completely converge to zero resulting in a certain degree of performance deterioration. The degree of the performance deterioration heavily depends upon the transition time of the input u and the magnitude of the imposed system uncertainties. It is also remarked that the control system given by Eq. (9) remains to be stable even with the semi active control input, due the fact that the semi-active controller only assures the increment of energy dissipation of the stable system.

5. Results and Discussion

The experimental apparatus for vibration control of the ER engine mount is presented in Fig. 5. Two non-contact proximitors (Bently Nevada 7200series) are used to measure the displacement of the engine mass and excitation, respectively. The excitation displacement is generated from the electromagnetic-type shaker. The data are stored in a micro-computer (IBM PC486) through an A/D (analog/digital) converter which has 12bits (DAS-1802H). The sampling frequency is chosen to be 1000Hz. Depending on the information of the displacement and velocity of the engine mass and excitation, the control electric field is determined and applied to the ER engine mount through the high voltage amplifier (Trek 10/

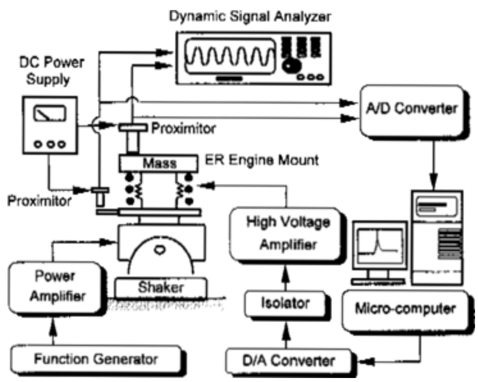

Fig. 5 Experimental apparatus of the ER engine mount test.

Table 1 Design and control parameters of the ER engine mount.

Engine mass (kg)	m	4
Stiffness of engine mount (N/m)	k_0	14,252
Damping of engine mount (N. s/m)	b_0	86
Electrode gap (mm)	h	1.5
Electrode length (mm)	L	30
Radius of electrodes (mm)	r_1	20.75
	r_2	24.25
	r_3	27.25
	r_4	30.75
Slope of sliding surface	C	2
Boundary layer width	ε	0.05
Weighting factor for stiffness	ρ_1	0.25
Weighting factor for damping	ρ_2	0.25
Bound value of excitation displacement	Ψ_1	0.0015
Bound value of excitation velocity	Ψ_2	0.3

10A) which has a gain of 1000. The design and control parameters of the proposed ER engine mount are given in Table 1.

In order to identify system parameters such as the nominal stiffness and damping of the ER engine mount, the frequency response analysis under random excitation is undertaken. In other words, by applying random excitation to the ER engine mount, we obtain frequency response ($|x/y|$) of the system. At this time, the excitation displacement is used as the input variable and the displacement of the engine mass as the output variable. Then, using curve fitting method based on the dynamic model of the ER engine mount given by Eq. (5), we determine the system parameters. Fig. 6 presents measured and curve fitted frequency responses of the ER engine mount at 0kV/mm. The maximum value of 2.95 takes place at the natural frequency. The natural frequency and damping ratio are estimated to be 9.5Hz and 0.18, respectively. From these data, the stiffness and the damping of the system are identified to be k_0=14,252N/m and b_0=86N. s/m, respectively.

We obtained vibration responses in frequency domain as shown in Fig. 7 which clearly shows that the imposed vibration is effectively suppressed at the neighborhood of resonance by applying constant field of 4kV/mm or sliding mode control (SMC) field. In constant field of 4kV/mm, the value at resonance frequency is reduced to 1.07 and, in SMC, the value is decreased to 1.21. However, we see that the SMC may provide better

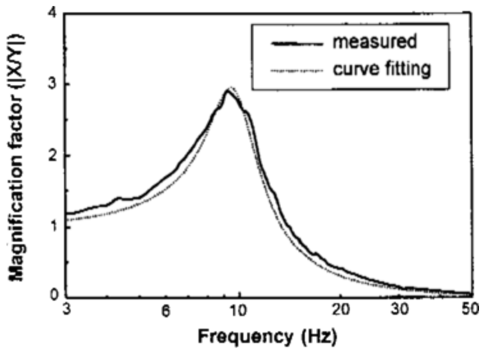

Fig. 6 Frequency response of the ER engine mount at 0kV/mm.

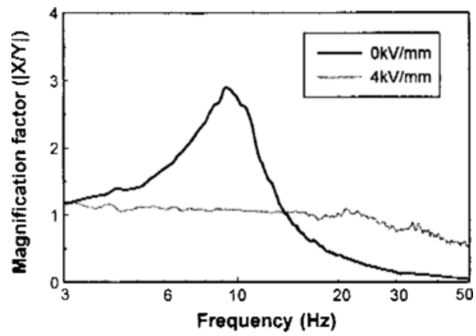

(a) Constant electric field

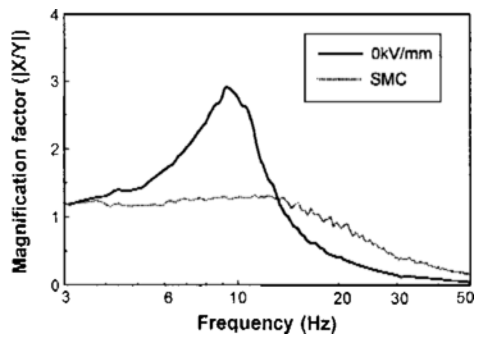

(b) Sliding mode control

Fig. 7 Frequency responses of the ER engine mount.

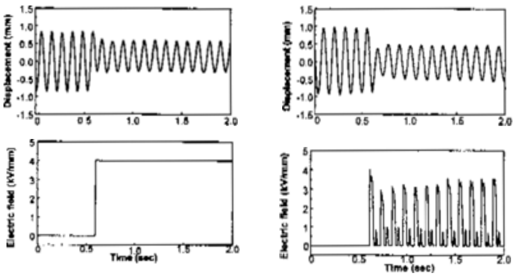

(a) Constant electric field (b) Sliding mode control

Fig. 8 Time responses of the ER engine mount under sinusoidal excitation.

response at relatively high frequency range (say, above 20Hz). In addition, we observe that performance deterioration due to the lock-up state, which normally takes place in the flow-mode ER engine mount, does not occur in either case. This is one of salient features of the proposed shear-mode ER engine mount. Fig. 8 shows control responses in time domain. The vibration is imposed to the frame of the ER engine mount by applying a sinusoidal excitation with the frequency of 9.0Hz and the magnitude of 0.4mm. It is also observed that the imposed vibration is quickly suppressed by applying the constant field of 4kV/mm or the sliding mode control field. However, we see that the suppressed displacement with the constant field of 4kV/mm is not symmetric with respect to zero value. This is mainly due to the field-dependent damping characteristics (frictional property) of the ER engine mount. To resolve this problem, a semi-active actuating condition should be employed by considering the direction of vibratory motion of the system. This is demonstrated by the sliding mode controller given by Eq. (12) with the semi-active condition given by Eq. (14). As expected, we see from Fig. 8(b) that the control electric field is supplied according to the semi-active fashion. The effectiveness of this control strategy is more clearly highlighted when the system vibrates under the random excitation. Fig. 9 presents control responses of the ER engine mount under the random excitation. We clearly observe that the control response with the constant field of 4kV/mm is worse than that with zero field, while the control response with the proposed sliding mode

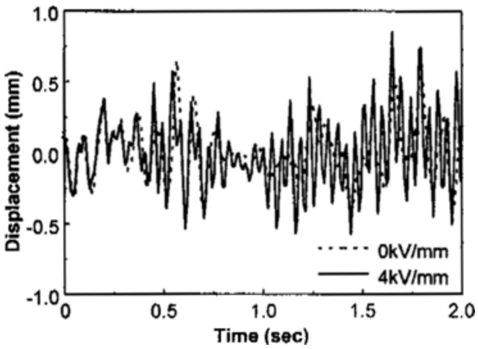

(a) Constant electric field

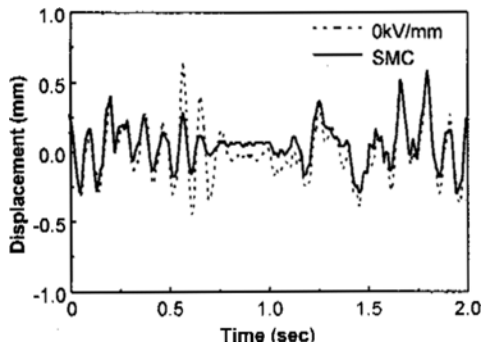

(b) Sliding mode control

Fig. 9 Time responses of the ER engine mount under random excitation.

controller is satisfactory. However, a great improvement of the vibration isolation performance does not take place. This is due to the fact that the dominant frequency component of the random excitation applied to the ER engine mount is relatively high (over 20Hz).

6. Conclusions

A new type of shear-mode ER engine mount was proposed and its feedback control characteristics were experimentally evaluated. First, the field-dependent yield shear stress of the arabic gum-based ER fluid was determined experimentally using a couette type electroviscometer. The field-dependent yield shear stress was then incorporated into the governing equation of motion of the ER engine mount. A sliding mode controller which has inherent robustness to system uncertainties was formulated and experimentally implemented to isolate the vibrations due to sinusoidal and random excitations. It has been shown that the vibration of the engine mass is significantly suppressed by employing the sliding mode controller with the semi-active actuating condition. In addition, the lock-up state which may deteriorate control performance in the relatively high frequency has not been occurred during control action of the proposed shear-mode ER engine mount. As a future study a hardware-in-the-loop-simulation (HILS) system is being constructed by considering a full-car model of passenger vehicles. In addition, the analytical evaluation of control performance deterioration due to semi-active condition will be undertaken.

Acknowledgment

This work was partially supported by the Korea Science and Engineering Foundation under Contract 961-1002-014-1. This financial support is gratefully acknowledged.

References

Choi, S. B., Cheong, C. C. and Shin, H. C., 1995, "Sliding Mode Control of Vibration in a Single-Link Flexible Arm with Parameter Variations," *Journal of Sound and Vibration*, Vol. 179, No. 5, pp. 737~748.

Choi, S. B. Choi, Y. T., Chang, E. G., Han, S. J. and Kim, C. S., 1998, "Control Characteristics of a Continuously Variable ER Damper," *Mechatronics*, Vol. 8, pp. 143~161.

Duclos, T. G., 1987, "An Externally Tunable Hydraulic Mount Which Uses Electro-Rheological Fluid," *SAE Technical Paper* 870963.

Jordan, T. C. and Shaw, M. T., 1989, "Electrorheology," IEEE *Transaction of Electrical Insulation*, Vol. 24, No. 5, pp. 849~878.

Leitmann, G., 1981, "On the Efficacy of Nonlinear Control in Uncertain Linear Systems," ASME *Journal of Dynamic Systems, Measurement, and Control*, Vol. 102, pp. 95~102.

Leitmann, G., 1994, "Semiactive Control for Vibration Attenuation," *Journal of Intelligent Material Systems and Structures*, Vol. 5, No. 5, pp. 841~846.

Morishita, S. and Mitsui, J., 1992, "An Electronically Controlled Engine Mount Using Electro-Rheological Fluid," *SAE Technical Paper* 922290.

Petek, N. K., Goudie, R. J. and Boyle, F. P., 1988, "Actively Controlled Damping in Electrorheological Fluid-Filled Engine Mounts," *SAE Technical Paper* 881785.

Rosenberg, R. C. and Karnopp, D. C., 1983, *Introduction to Physical System Dynamics*, McGraw-Hill, New York.

Ushijima, T, Takano, K. and Kojima, H., 1988, "High Performance Hydraulic Mount for Improving Vehicle Noise and Vibration," *SAE Technical Paper* 880073.

Williams, E. W., Rigby, S. G., Sproston, J. L. and Stanway, R., 1993, "Electrorheological Fluids Applied to An Automotive Engine Mount," *Journal of Non-Newtonian Fluid Mech.*, Vol. 47, pp. 221~238.